JOC Article

[12]Annulene Radical Anions Revisited: Evaluation of Structure Assignments Based on Computed Energetic and Electron Spin Resonance Data

Miles N. Braten,[†] M. Gertrude Gutierrez,[†] Claire Castro,*[,†] and William L. Karney*[,†,‡]

Departments of Chemistry and Environmental Science, University of San Francisco, 2130 Fulton Street, San Francisco, California 94117

castroc@usfca.edu; karney@usfca.edu

Received June 11, 2008

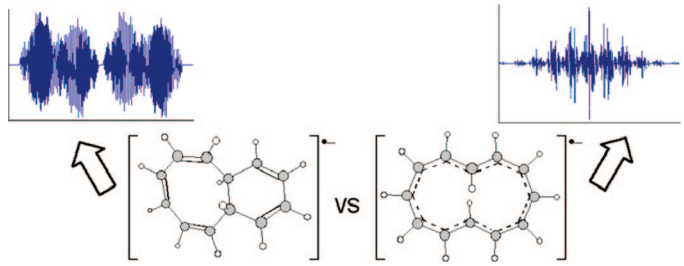

We report density functional and coupled cluster calculations on numerous monocyclic and bicyclic $(CH)_{12}^{\bullet-}$ isomers. At the RCCSD(T)/cc-pVDZ//UB3LYP/6-31+G* level, a nearly planar, bond-equalized radical anion of 1,7-di-*trans*-[12]annulene (**4a**$^{\bullet-}$) is lowest in energy; several other isomers and conformations lie within 3 kcal/mol of **4a**$^{\bullet-}$. RCCSD(T)/AUG-cc-pVDZ//UB3LYP/6-31+G* results place the all-cis isomer **3**$^{\bullet-}$ slightly below **4a**$^{\bullet-}$ in energy. Validation studies on the heptalene radical anion, [16]annulene radical anion, and tri-*trans*-[12]annulene radical anion indicate that electron spin resonance (ESR) hyperfine coupling constants (a_H values) computed at the BLYP/EPR-III level on DFT geometries give much better agreement with experimental values than those computed using B3LYP/6-31G*. We were unable to locate any $C_{12}H_{12}^{\bullet-}$ isomer that could account for the ESR spectrum previously attributed to a highly twisted structure for the 1,7-di-*trans*-[12]annulene radical anion. Our computed energetic and ESR data for [12]annulene radical anions and their valence isomers suggest that **4a**$^{\bullet-}$ may have been made, yet its ESR spectrum was incorrectly assigned to the bicyclic isomer **6b**$^{\bullet-}$. Finally, the computed ^{1}H NMR shift values of the dianion of **4** reveal a distinct diatropic ring current that should aid in its characterization.

Introduction

Unlike neutral annulenes, which have received considerable attention from both experimentalists and theoreticians in recent years,[1] annulene radical anions are less well studied. Yet understanding their structures and reactivity is important for a variety of reasons. In addition to their unusual structures, radical ions offer potential routes to species that are difficult to access via the corresponding neutral potential surface. Their reactivity can differ dramatically as a result of the extra electron, in some cases even inverting the potential energy profile for a reaction.[2] Moreover, photoelectron spectroscopy of radical anions has led to information about transition states for dynamic processes.[3] The use of electron spin resonance (ESR) spectroscopy to characterize these species has also prompted improvements in the direct computation of ESR parameters such as hyperfine coupling constants, with the goal of making more reliable structural assignments.[4]

Several radical anions of [4*n*]annulenes[5−8] (and [4*n*+2]annulenes[9,10]) have been investigated by ESR spectroscopy. In general, the neutral parent annulenes were first characterized by NMR spectroscopy before the corresponding radical anions were generated. A recent exception to this was the synthesis of the di-*trans*-[12]annulene radical anion reported by Stevenson and co-workers (Scheme 1).[8a] Although no NMR data were obtained, the presence of this highly reactive [12]annulene was

[†] Department of Chemistry.
[‡] Department of Environmental Science.
(1) Spitler, E. L.; Johnson, C. A.; Haley, M. M. *Chem. Rev.* **2006**, *106*, 5344.

10.1021/jo801249t CCC: $40.75 © 2008 American Chemical Society
Published on Web 10/22/2008

SCHEME 1

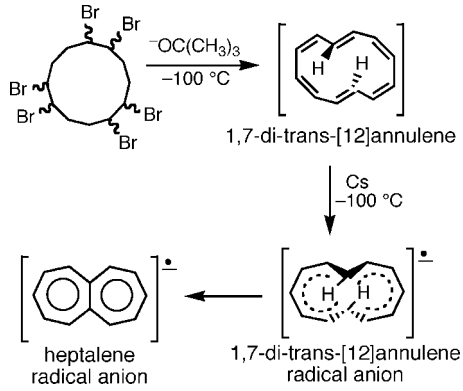

inferred by the ESR spectrum attributed to the radical anion resulting from immediate reduction of an undetected neutral species. The combination of the ESR data, density functional theory calculations (B3LYP/6-31G*), and the formation of the heptalene radical anion upon warming led to the assignment of the ESR spectrum to the 1,7-di-*trans*-[12]annulene radical anion. The small total spectral width (13.5 G) suggested a very nonplanar conformation.[8,11]

Given the unknown stereochemistry of the starting material, 1,2,5,6,9,10-hexabromocyclododecane, and considering the variety of E2 and E2′ pathways available, it seemed possible that other isomers of $C_{12}H_{12}$ might have been produced. Prior computational work on neutral [12]annulene isomers predicted that several structures, including mono-*trans*-[12]annulene (**1**), tri-*trans*-[12]annulene (**2**), and the all-*cis*-[12]annulene **3**, are more stable than the 1,7-di-*trans* species **4** (Figure 1).[12] In addition, the bicyclic $C_{12}H_{12}$ isomers **6a** and **6b** (*cis*/*trans*-bicyclo[6.4.0]dodeca-2,4,6,9,11-pentaene) are considerably more stable than any monocyclic system (Figure 1). However, the relative ordering of the radical anions might be different from that of their neutral counterparts.

ESR spectroscopy is often employed to extract information about spin densities in conjugated systems. Conversely, computed spin densities are sometimes used to help assign observed ESR spectra to particular structures. For planar π-radicals, the McConnell relationship[13] (eq 1) relates a_H values (hyperfine

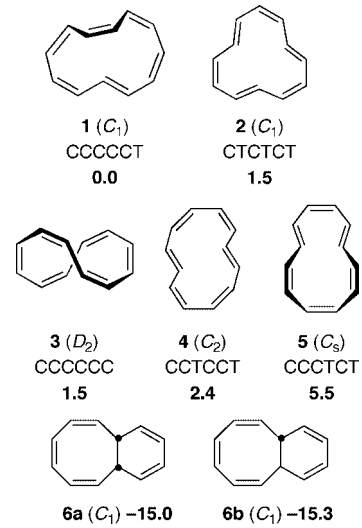

FIGURE 1. Low-lying neutral [12]annulene isomers and isomeric ring closure products previously identified computationally. Relative energies (kcal/mol) computed using CCSD(T)/cc-pVDZ//BHHLYP/6-311+G** + ZPE. *Cis*−*trans* configurations are shown. Data from ref 12.

coupling constants) to π-spin densities (ρ) on specific carbon atoms, where Q is the proportionality constant.

$$a_H = Q\rho \quad (1)$$

For the radical anions of cyclooctatetraene (COT) and [16]annulene, Q is 25.7[5] and 24.8 G,[6] respectively, well within the range of 22−27 Gauss common for planar conjugated hydrocarbons. According to eq 1, a large coupling constant translates to a large π-spin density on the corresponding carbon. Values of Q smaller than 22−27 G are commonly viewed as indicative of nonplanarity. This is exemplified by the tri-*trans*-[12]annulene radical anion, for which Q and the total spectral width are 9.8 G.[7] As stated above, the argument in favor of the very nonplanar structure of the reported 1,7-di-*trans*-[12]annulene radical anion was the very small spectral width, 13.5 G.

The simplicity of the synthesis of the 1,7-di-*trans*-[12]annulene radical anion and the possibility that other [12]annulene/[12]annulene$^{\bullet-}$ isomers might be accessible via this and similar routes[8b] motivated us to computationally study the $C_{12}H_{12}^{\bullet-}$ hypersurface and to compute ESR hyperfine coupling constants to aid in the characterization of these highly reactive species. Since the species of interest contain both sp^2 and sp^3 (bridgehead) carbons, we focused on computing accurate a_H values (not spin densities) and comparing them with empirically determined ones. (The McConnell relationship does not apply to radicals that have sp^3 carbons.) In addition, one of our methodological goals was to determine whether the caveats regarding the use of B3LYP for neutral annulenes (e.g., sensitivity of computed magnetic properties to geometry, erroneous energy ordering, vide infra) also apply to the annulene radical anions.

Computational Methods

Geometries of stationary points were optimized using unrestricted density functional theory (UDFT), including the B3LYP,[14] BLYP,[14b,15] and BHHLYP[16] functionals. These optimizations employed the 6-31G*, 6-31+G*, and 6-311+G** basis sets.[17] Vibrational analyses were performed at the same level as the geometry optimizations, to verify that species were either minima (no imaginary frequencies) or transition states (one imaginary), and

(2) Hammad, L. A.; Wenthold, P. G. *J. Am. Chem. Soc.* **2003**, *125*, 10796.
(3) Wenthold, P. G.; Hrovat, D. A.; Borden, W. T.; Lineberger, W. C. *Science* **1996**, *272*, 1456.
(4) *Calculation of NMR and EPR Parameters: Theory and Applications*; Kaupp, M., Bühl, M., Malkin, V. G., Eds.; Wiley-VCH: Weinheim, 2004.
(5) (a) Katz, T. J.; Strauss, H. L. *J. Chem. Phys.* **1960**, *32*, 1873. (b) Strauss, H. L.; Katz, T. J.; Fraenkel, G. K. *J. Am. Chem. Soc.* **1963**, *85*, 2360. (c) Carrington, A.; Todd, P. F. *Mol. Phys.* **1963**, *7*, 533.
(6) (a) Oth, J. F. M.; Baumann, H.; Gilles, J.-M.; Schröder, G. *J. Am. Chem. Soc.* **1972**, *94*, 3498. (b) Concepcion, J. G.; Vincow, G. *J. Phys. Chem.* **1975**, *79*, 2037. (c) Stevenson, G. R.; Reiter, R. C.; Sedgwick, J. B. *J. Am. Chem. Soc.* **1983**, *105*, 6521.
(7) Stevenson, G. R.; Concepcion, R.; Reiter, R. C. *J. Org. Chem.* **1983**, *48*, 2777.
(8) (a) Gard, M.; Reiter, R. C.; Stevenson, C. D. *Org. Lett.* **2004**, *6*, 393. (b) Kiesewetter, M. K.; Gard, M. N.; Reiter, R. C.; Stevenson, C. D. *J. Am. Chem. Soc.* **2006**, *128*, 15618. (c) Stevenson, C. D. *Acc. Chem. Res.* **2007**, *40*, 703.
(9) (a) Tuttle, T. R., Jr.; Weissman, S. I. *J. Am. Chem. Soc.* **1958**, *80*, 5342. (b) Fessenden, R. W.; Ogawa, S. *J. Am. Chem. Soc.* **1964**, *86*, 3591.
(10) (a) Kurth, T. L.; Brown, E. C.; Hattan, C. M.; Reiter, R. C.; Stevenson, C. D. *J. Phys. Chem. A* **2002**, *106*, 478. (b) Oth, J. F. M.; Woo, E. P.; Sondheimer, F. *J. Am. Chem. Soc.* **1973**, *95*, 7337.
(11) For the impact of nonplanarity on EPR hyperfine coupling constants in bridged [14]annulenes, see: Gerson, F.; Müllen, K.; Vogel, E. *J. Am. Chem. Soc.* **1972**, *94*, 2924.
(12) Braten, M. N.; Castro, C.; Herges, R.; Köhler, F.; Karney, W. L. *J. Org. Chem.* **2008**, *73*, 1532.
(13) McConnell, H. M. *J. Chem. Phys.* **1956**, *24*, 632.

to obtain zero-point corrections. On the basis of agreement between computed and observed hyperfine coupling constants for reference species (vide infra) and on the fact that B3LYP geometries gave the lowest CCSD(T) absolute energies, the B3LYP/6-31+G* geometries were used for key species here.

For neutral annulenes, many DFT methods (including B3LYP) give erroneous relative energies and sometimes qualitatively incorrect energy ordering of isomers.[18,19] In addition, B3LYP does very poorly when comparing monocyclic and bicyclic isomers.[20] When feasible, coupled cluster theory—in particular the CCSD(T) method[21]—is often considered the method of choice for determination of relative energies.[20] Thus, using the B3LYP/6-31+G* optimized geometries, energies were recomputed at the UCCSD(T)/6-31+G** level. In accord with earlier studies on conjugated π radicals,[22] the UCCSD(T) results were prone to high spin contamination ($<S^2> > 1.0$ for many of the species), even after annihilation of the first spin contaminant (see Supporting Information, Table S1). For this reason, single-point energies were also obtained using restricted open-shell coupled cluster theory, at the RCCSD(T)/cc-pVDZ level,[23,24] which avoids spin contamination. For selected species, RCCSD(T) energies were determined with the AUG-cc-pVDZ basis set, which includes diffuse functions on all atoms. Due to resource limitations, these latter calculations were not possible for isomers without any symmetry.

For a given class of radicals, it is important to find the method that works best for calculating hyperfine coupling constants.[4] This has not yet been done for annulene radical anions. Thus, for validation purposes, a_H values were computed for several reference systems using the B3LYP, BHHLYP, and BLYP methods with a variety of basis sets, including 6-31G*, 6-31+G*, 6-311+G**, and the EPR-III basis set of Barone.[25] The latter basis set includes diffuse functions and polarization functions on both carbon and hydrogen. For $C_{12}H_{12}^{\bullet-}$ isomers, the EPR-III basis set was used.[26]

NMR chemical shifts were computed at the GIAO-B3LYP/6-31+G*//B3LYP/6-31+G* level and were referenced to TMS. DFT and UCCSD(T) calculations were performed using Gaussian 03.[27] RCCSD(T) calculations were done with MOLPRO.[28] Structures were visualized with MacMolPlt,[29] and MOs were visualized using Molden.[30] ESR spectra were simulated with the WinSim software[31] using a line width of 0.05 G. Varying the line width in the range 0.04−0.08 G caused very little change in the appearance of the simulated spectra.

Results and Discussion

Method Validation for Hyperfine Coupling Constants. While other groups have reported methods for computing isotropic hyperfine coupling constants (a_H) for organic radical anions,[22a,32] these studies did not focus on annulenes.[33] Isotropic hyperfine coupling constants at several levels for the heptalene radical anion and [16]annulene radical anion are presented in Table 1. We chose heptalene$^{\bullet-}$ as our initial benchmark as it is the final product presented in Scheme 1 and has been previously well characterized by Müllen.[34] The research by different groups[6] on [16]annulene$^{\bullet-}$ made it our choice for referencing computed a_H values for a delocalized but still nonplanar annulene system. Finally, although not as well studied as [16]annulene$^{\bullet-}$, we also include representative computed a_H values for the bond alternating tri-*trans*-[12]annulene$^{\bullet-}$ (**2**$^{\bullet-}$) (Table 2).[7]

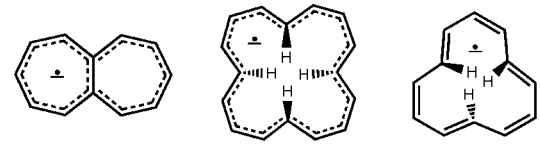

heptalene$^{\bullet-}$ D_{2h} [16]annulene$^{\bullet-}$ D_{2d} [12]annulene$^{\bullet-}$ C_1

From the data on all three species, it becomes clear that the choice of functional for computing a_H values seems more important than the method for optimizing the geometry, with BLYP superior to both B3LYP and BHHLYP. For example, B3LYP/6-31G*// provides a total spectral width consistently too large: heptalene$^{\bullet-}$, 34.6 vs 25.7 G (exptl); [16]annulene$^{\bullet-}$, 61.6 vs 38.5 G (exptl); and tri-*trans*-12]annulene$^{\bullet-}$ 19.0 vs 9.8 G (exptl). This is noteworthy because B3LYP/6-31G*// was used to compute carbon spin densities for [12]annulene radical anions.[8] By comparison, simply switching to BLYP/6-31G*// B3LYP/6-31G* improved the results dramatically: computed spectral widths for the same species become 26.1, 42.7, and 14.1 G, respectively. Thus, unlike Batra et al., who found B3LYP and BLYP to give comparable results,[32a] we find BLYP to be consistently superior for a_H values.

While BLYP performed best for computing a_H, the choice of basis set to pair with this functional was not as clear. For heptalene$^{\bullet-}$, BLYP results for coupling constants are relatively insensitive to the basis set used, with 6-31+G* and EPR-III slightly better than 6-31G*. However, for [16]annulene$^{\bullet-}$, the EPR-III basis set clearly gives the best agreement with experiment, for both individual a_H values and total spectral width (last three entries). The BLYP results on tri-*trans*-[12]annulene$^{\bullet-}$

(14) (a) Becke, A. D. *J. Chem. Phys.* **1993**, *98*, 5648. (b) Lee, C.; Yang, W.; Parr, R. G. *Phys. Rev. B* **1988**, *37*, 785.
(15) Becke, A. D. *Phys. Rev. A.* **1988**, *38*, 3098.
(16) (a) Becke, A. D. *J. Chem. Phys.* **1992**, *98*, 1372. (b) Miehlich, B.; Savin, A.; Stoll, H.; Preuss, H. *Chem. Phys. Lett.* **1989**, *157*, 200.
(17) Hariharan, P. C.; Pople, J. A. *Theor. Chim. Acta* **1973**, *28*, 213.
(18) (a) King, R. A.; Crawford, T. P.; Stanton, J. F.; Schaefer, H. F. *J. Am. Chem. Soc.* **1999**, *121*, 10788. (b) Wannere, C. S.; Sattelmeyer, K. W.; Schaefer, H. F.; Schleyer, P. v. R. *Angew. Chem., Int. Ed.* **2004**, *43*, 4200.
(19) Castro, C.; Karney, W. L.; McShane, C. M.; Pemberton, R. P. *J. Org. Chem.* **2006**, *71*, 3001.
(20) (a) Schreiner, P. R.; Fokin, A. A.; Pascal, R. A.; de Mejere, A. *Org. Lett.* **2006**, *8*, 3635. (b) Wodrich, M. D.; Corminboeuf, C.; Schreiner, P. R.; Fokin, A. A.; Schleyer, P. v. R. *Org. Lett.* **2007**, *9*, 1851.
(21) (a) Bartlett, R. J. *J. Phys. Chem.* **1989**, *93*, 1697. (b) Raghavachari, K.; Trucks, G. W.; Pople, J. A.; Head-Gordon, M. *Chem. Phys. Lett.* **1989**, *157*, 479. (c) Scuseria, G. E. *Chem. Phys. Lett.* **1991**, *176*, 27.
(22) (a) Bally, T.; Hrovat, D. A.; Borden, W. T. *Phys. Chem. Chem. Phys.* **2000**, *2*, 3363. (b) Bally, T.; Borden, W. T. *Reviews in Computational Chemistry*; Lipkowitz, K. B., Boyd, D. B., Eds.; Wiley: New York, 1999; Vol. 13.
(23) (a) Knowles, P. J.; Hampel, C.; Werner, H.-J. *J. Chem. Phys.* **1993**, *99*, 5219 (Erratum, *J. Chem. Phys.* **2000**, *112*, 3106). (b) Watts, J. D.; Gauss, J.; Bartlett, R. J. *J. Chem. Phys.* **1993**, *98*, 8718.
(24) Dunning, T. H., Jr. *J. Chem. Phys.* **1989**, *90*, 1007.
(25) Rega, N.; Cossi, M.; Barone, V. *J. Chem. Phys.* **1996**, *105*, 11060.
(26) The effect of solvation on computed a_H values was also investigated in the case of heptalene. Using the SCI-PCM model and specifying tetrahydrofuran as solvent, there was no significant change in the computed a_H values. (See Supporting Information.) Thus, solvation-based calculations were not pursued for other species.
(27) Frisch, M. J. et al. *Gaussian 03*, revision D.01; Gaussian, Inc.: Wallingford, CT, 2004.
(28) Werner, H.-J.; Knowles, P. J.; Lindh, R.; Manby, F. R.; Schütz, M.; Celani, P.; Korona, T.; Rauhut, G.; Amos, R. D.; Bernhardsson, A.; Berning, A.; Cooper, D. L.; Deegan, M. J. O.; Dobbyn, A. J.; Eckert, F.; Hampel, C.; Hetzer, G.; Lloyd, A. W.; McNicholas, S. J.; Meyer, W.; Mura, M. E.; Nicklass, A.; Palmieri, P.; Pitzer, R.; Schumann, U.; Stoll, H.; Stone, A. J.; Tarroni, R.; Thorsteinsson, T. *MOLPRO*, version 2006.1. See http://www.molpro.net.
(29) MacMolPlt v.5.3.5: Bode, B. M.; Gordon, M. S. *J. Mol. Graphics Modeling* **1998**, *16*, 133.
(30) Schaftenaar, G.; Noordik, J. H. *J. Comput.-Aided Mol. Design* **2000**, *14*, 123.
(31) Duling, D. R. *J. Magn. Reson., Ser. B* **1994**, *104*, 105.
(32) (a) Batra, R.; Giese, B.; Spichty, M.; Gescheidt, G.; Houk, K. N. *J. Phys. Chem.* **1996**, *100*, 18371. (b) Gauld, J. W.; Eriksson, L. A.; Radom, L. *J. Phys. Chem. A* **1997**, *101*, 1352.
(33) An exception to this is the COT radical anion, which has been studied both experimentally[5] and computationally.[38]
(34) Müllen, K. *Helv. Chim. Acta* **1974**, *57*, 2399.

TABLE 1. Comparison of Experimental and Calculated ESR Hyperfine Coupling Constants and Spectral Widths (Gauss) for Radical Anions of Heptalene (D_{2h}) and [16]annulene (D_{2d})

method (heptalene$^{\bullet-}$)[a]	a_H1 (4H)	a_H2 (2H)	a_H3 (4H)	sp. width
BHHLYP/6-31+G*// BHHLYP/6-31+G*	−9.01	3.27	2.65	53.18
BHHLYP/6-311+G**// BHHLYP/6-311+G**	−8.09	2.93	2.37	47.70
BHHLYP/EPR-III// BHHLYP/6-311+G**	−6.11	1.42	0.92	30.96
B3LYP/6-31G*// B3LYP/6-31G*	−6.77	1.61	1.08	34.62
B3LYP/6-31+G*// B3LYP/6-31+G*	−6.56	1.52	1.00	33.28
B3LYP/6-311+G**// B3LYP/6-311+G**	−5.84	1.35	0.88	29.58
B3LYP/6-311+G**// BHHLYP/6−31+G*	−5.82	1.33	0.88	29.46
B3LYP/6-311+G**// BHHLYP/6-311+G**	−5.80	1.32	0.87	29.32
B3LYP/EPR-III// B3LYP/6-31+G*	−6.20	1.47	0.95	31.54
B3LYP/EPR-III// B3LYP/6-311+G**	−6.17	1.45	0.94	31.34
BLYP/6-31G*// B3LYP/6-31G*	−5.67	0.90	0.40	26.08
BLYP/6-31G*// BLYP/6-31G*	−5.71	0.91	0.41	26.30
BLYP/6-31+G*// BLYP/6-31+G*	−5.53	0.86	0.36	25.26
BLYP/EPR-III// BHHLYP/6-31+G*	−5.13	0.80	0.33	23.44
BLYP/EPR-III// B3LYP/6-31G*	−5.17	0.81	0.33	23.62
BLYP/EPR-III// BLYP/6-31+G*	−5.22	0.82	0.33	23.86
BLYP/EPR-III// B3LYP/6-31+G*	−5.18	0.81	0.33	23.66
EXPERIMENT[b]	**−5.35**	**0.79**	**0.69**	**25.74**
method ([16]annulene$^{\bullet-}$)	a_H1 (8H)	a_H2 (4H)	a_H3 (4H)	sp. width
B3LYP/6-31G*// B3LYP/6-31G*	−5.58	2.37	1.86	61.6
B3LYP/6-31+G*// B3LYP/6-31+G*	−5.46	2.03	1.77	58.9
B3LYP/6-311+G**// B3LYP/6-311+G**	−4.87	1.74	1.61	52.4
BLYP/6-31G*// B3LYP/6-31G*	4.35	1.05	0.92	42.7
BLYP/6-31+G*// BLYP/6-31+G*	−4.28	1.01	0.87	41.8
BLYP/EPR-III// BHHLYP/6-31+G*	−3.92	0.99	0.81	38.5
BLYP/EPR-III// BLYP/6-31+G*	−4.04	0.98	0.84	39.6
BLYP/EPR-III// B3LYP/6-31+G*	−4.00	0.97	0.82	39.2
EXPERIMENT[c]	**−3.96**	**0.96**	**0.74**	**38.5**

[a] For a more complete set of data on heptalene, see Supporting Information. [b] Data from ref 8 and 34. [c] Data from ref 6.

(Table 2) suggest that both 6-31+G* and EPR-III perform well for a_H values, but EPR-III does better in computing total spectral width.

As an additional test of the method, BLYP/EPR-III//B3LYP/6-31+G* calculations on the COT radical anion give $a_H = 3.04$ G for all eight hydrogens, in good agreement with the experimental value of 3.21 G obtained by Katz and Strauss.[5a]

Finally, the problems associated with using B3LYP geometries for computing magnetic (e.g., NMR) properties of neutral annulenes are not apparent here in ESR data for radical anions.

TABLE 2. Comparison of Experimental and Calculated a_H values (Gauss) of the Tri-*trans*-[12]annulene Radical Anion

method	a_H1 (3H)	a_H2 (3H)	a_H3 (6H)	sp. width
B3LYP/6-31G*// B3LYP/6-31G*	− 2.36	− 2.69	0.65	19.05
B3LYP/6-31+G*// B3LYP/6-31+G*	− 1.96	− 2.33	0.45	15.57
BLYP/6-31G*// B3LYP/6-31G*	−1.65	− 1.94	0.56	14.13
BLYP/6-31+G*// BLYP/6-31+G*	−1.47	−1.80	0.32	11.70
BLYP/EPR-III// BHHLYP/6-31+G*	−1.10	−1.35	0.54	10.59
BLYP/EPR-III// B3LYP/6-31G*	−1.22	−1.46	0.64	11.88
BLYP/EPR-III// B3LYP/6-31+G*	−1.14	−1.39	0.55	10.89
EXPERIMENT[a]	**1.30**	**1.53**	**0.225**	**9.84**

[a] Although the molecule has C_1 symmetry, the fast interconversion of the internal protons on the ESR time scale renders the molecule as having effective D_{3d} symmetry. Data from ref 7.

For a_H values calculated at the BLYP/EPR-III level, both BHHLYP/6-31+G* and B3LYP/6-31+G* geometries give comparable results.

In sum, based on the data from all three systems, BLYP/EPR-III provides consistently good agreement with experimental a_H values and total spectral widths, when used with either B3LYP/6-31+G* or BHHLYP/6-31+G* geometries. In contrast to neutral annulenes, for which BHHLYP gives better geometries for evaluating magnetic properties, for the radical anions the strong tendency toward delocalization diminishes the difference between B3LYP and BHHLYP geometries.

Structures and Relative Energies. The B3LYP/6-31+G* optimized geometries for the most stable conformations of the radical anions of **1**−**5** are shown in Figure 2. Table 3 provides energetic data for these and other $C_{12}H_{12}$ radical anion isomers. Several key results emerge from the data in Table 3. For **1**$^{\bullet-}$ to **5**$^{\bullet-}$, the relative ordering at RCCSD(T)/cc-pVDZ is the same as that obtained with UB3LYP (**4a**$^{\bullet-}$ > **2**$^{\bullet-}$ > **3**$^{\bullet-}$ > **1**$^{\bullet-}$ > **5**$^{\bullet-}$, least stable), though the differences are much smaller with RCCSD(T). At this level of theory, the three most stable isomers differ by less than 2 kcal/mol. The main change in relative energy ordering when compared with the neutral species (**1** > **2** ∼ **3** > **4** > **5**), is the switch between mono-*trans* and 1,7-di-*trans* isomers. This is possibly due to the ability of **4a**$^{\bullet-}$ to adopt an especially planar conformation (not available in the neutral species) that can more effectively delocalize the charge. We were unable to locate any corresponding delocalized conformational minima for species **1**$^{\bullet-}$, **2**$^{\bullet-}$, **3**$^{\bullet-}$, and **5**$^{\bullet-}$. In fact, the only minima located for these species were those analogous to the conformations adopted by their neutral counterparts. Lastly, considering only the species shown in Figure 2, bicyclic isomers **6a**$^{\bullet-}$ and **6b**$^{\bullet-}$are higher in energy than several of the monocyclic radical anions. This is in sharp contrast to the neutral PES, where the bicyclic isomers **6a** and **6b** are thermodynamic sinks (Figure 1).[35]

The RCCSD(T) results discussed above employed the cc-pVDZ basis set, which does not have diffuse functions. To determine the effect of diffuse functions on relative energies, RCCSD(T)/AUG-cc-pVDZ energies were computed for all species with at least one symmetry element. (Such calculations were not possible for **1**$^{\bullet-}$, **2**$^{\bullet-}$, **6a**$^{\bullet-}$, or **6b**$^{\bullet-}$.) At this level, the range of relative energies is smaller, and at least three species

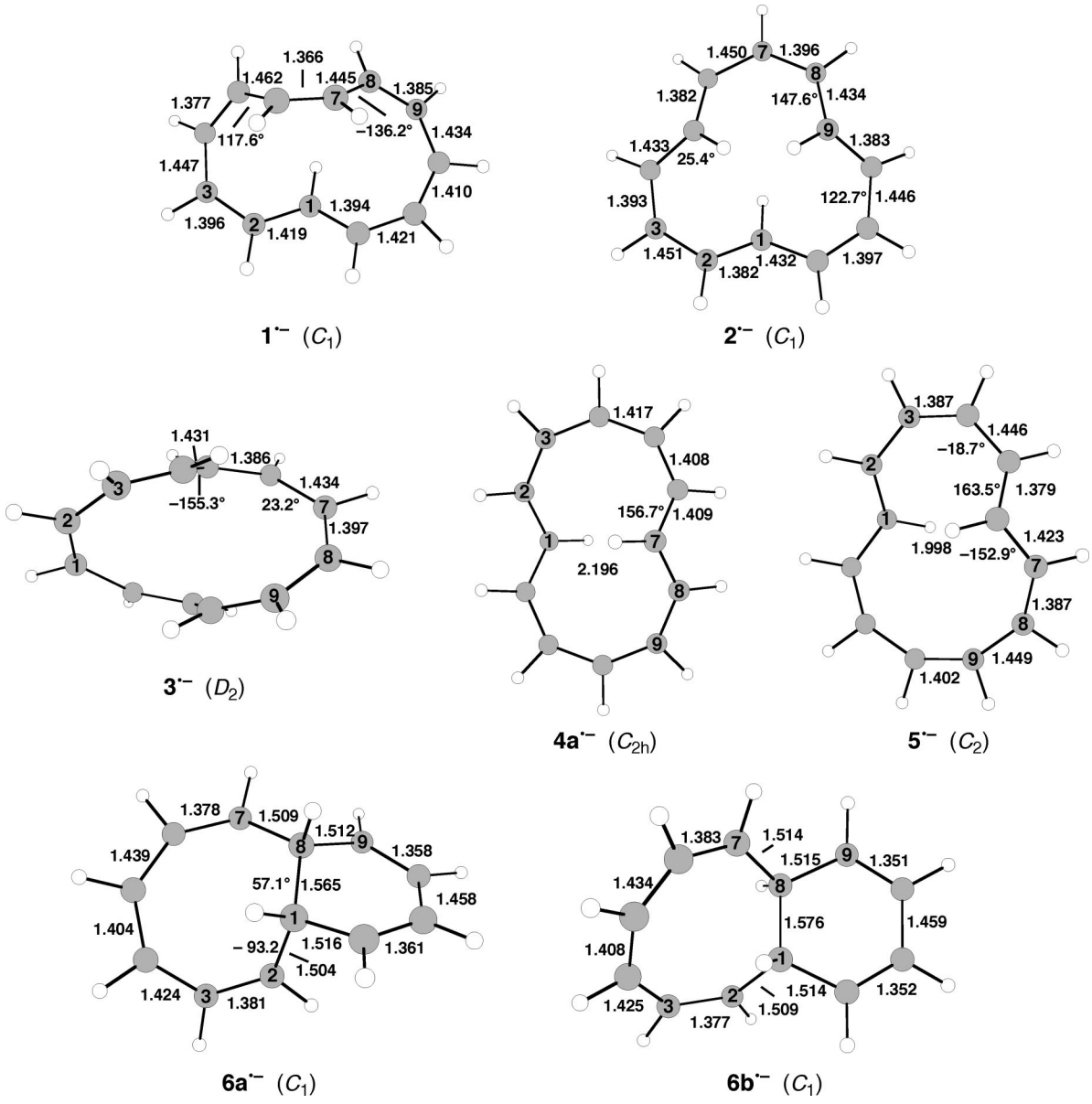

1$^{\bullet-}$ (C_1) **2**$^{\bullet-}$ (C_1)

3$^{\bullet-}$ (D_2) **4a**$^{\bullet-}$ (C_{2h}) **5**$^{\bullet-}$ (C_2)

6a$^{\bullet-}$ (C_1) **6b**$^{\bullet-}$ (C_1)

FIGURE 2. Optimized geometries (B3LYP/6-31+G*) of the most stable conformations of radical anions **1**$^{\bullet-}$−**6**$^{\bullet-}$. Distances in Å, selected CCCC dihedral angles in degrees. For **4a**$^{\bullet-}$ and **5**$^{\bullet-}$, the distances between the inner hydrogens are also given.

lie within 0.6 kcal/mol of the lowest isomer, **3**$^{\bullet-}$ (Table 3), including bicyclic isomer **8**$^{\bullet-}$ (vide infra).

Of the monocyclic species in Figure 2, di-*trans* **4a**$^{\bullet-}$, is unique in that it is fully bond-equalized; all the others retain bond-length alternation.[36,37] Unlike COT$^{\bullet-}$, which is planar but bond-alternating,[38] and **2**$^{\bullet-}$, which is more planar than its neutral counterpart but remains bond-alternating, **4a**$^{\bullet-}$ is the smallest [4*n*]annulene radical anion predicted to be bond-equalized. In this sense **4a**$^{\bullet-}$ resembles [16]annulene$^{\bullet-}$, for which a delocalized D_{2d}-symmetric structure is predicted to be a minimum, and should thus have a comparable spectral width (ca. 40 G). This prediction is at odds with the ESR spectrum assigned[8] to 1,7-di-*trans*-[12]annulene$^{\bullet-}$, which is very narrow (13.5 G). On the other hand, the computed energetics for both di-*trans* **4** and **4a**$^{\bullet-}$ support the possibility of their synthesis. To address this contradiction, we calculated ESR hyperfine coupling constants for **4a**$^{\bullet-}$ and other $C_{12}H_{12}^{\bullet-}$ isomers.

Hyperfine Coupling Constants for $C_{12}H_{12}^{\bullet-}$ Species. Table 4 lists the computed a_H values for the radical anions **1**$^{\bullet-}$, **3**$^{\bullet-}$, **4a**$^{\bullet-}$, **5**$^{\bullet-}$, and **6**$^{\bullet-}$, as well as the experimentally determined a_H values assigned to the 1,7-di-*trans*-[12]annulene radical anion. (For values for **2**$^{\bullet-}$, see Table 2.) There is no obvious match between these computed values and the experimental ones. For **4a**$^{\bullet-}$, the computed spectral width is 49 G, much larger than the experimental value (13.5 G). Although the least stable isomer, 1,5-di-*trans* **5**$^{\bullet-}$, has a computed narrow spectral width (14.3 G), its computed a_H values differ significantly from the experimental ones. The more stable isomer, all-*cis* **3**$^{\bullet-}$, also has

(35) One fundamental quantity for the species considered here is the electron attachment energy. To date, we have been unable to determine these at the RCCSD(T) level with a basis set that includes diffuse functions. Our preliminary results suggest, however, that **6a**$^{\bullet-}$ and **6b**$^{\bullet-}$ are, at best, weakly bound, especially compared to all the monocyclic species considered here. Further investigations in this area are in progress.

(36) Bond-equalized **4a**$^{\bullet-}$ has one imaginary frequency, corresponding to bond shifting that leads to a slightly more bond-alternating form, **4a-alt**$^{\bullet-}$. After correction for zero-point energy differences, however, **4a-alt**$^{\bullet-}$ is computed to be 0.2 kcal/mol higher than **4a**$^{\bullet-}$.

TABLE 3. Relative Energies (kcal/mol) for [12]Annulene Radical Anions and Bicyclic Valence Isomers[a]

				UB3LYP/6-31+G*			RCCSD(T)/cc-pVDZ	RCCSD(T)/AUG-cc-pVDZ
species	sym	state	config[b]	rel E	NI	$<S^2>$ before/after	rel E	rel E
monocyclic								
1$^{\bullet-}$	C_1	^{2}A	CCCCCT	8.0	0	0.763/0.750	4.7	——
2$^{\bullet-}$	C_1	^{2}A	CTCTCT	5.1	0	0.755/0.750	1.2	——
3$^{\bullet-}$	D_2	^{2}A	CCCCCC	6.9	0	0.754/0.750	1.7	−0.3
4a$^{\bullet-}$	C_{2h}	^{2}B$_g$	CCTCCT	0.0	1	0.787/0.751	0.0	0.0
4a-alt$^{\bullet-}$	C_i	^{2}A$_g$	CCTCCT	0.7	0	0.775/0.751	0.2	0.3
4b$^{\bullet-}$	D_2	^{2}B$_1$	CCTCCT	9.9	0	0.754/0.750	4.7	3.1
4c$^{\bullet-}$	C_2	^{2}B	CCTCCT	8.3	0	0.757/0.750	7.7	8.1
4d$^{\bullet-}$	C_2	^{2}B	CCTCCT	16.6	0	0.759/0.750	12.1	10.7
5$^{\bullet-}$	C_2	^{2}A	CCCTCT	11.5	0	0.755/0.750	10.6	11.4
bicyclic								
6a$^{\bullet-}$	C_1	^{2}A	cis	14.8	0	0.761/0.750	6.9	——
6b$^{\bullet-}$	C_1	^{2}A	trans	11.3	0	0.761/0.750	3.6	——
7a$^{\bullet-}$	C_2	^{2}B	trans	14.1	0	0.771/0.750	9.9	8.3
7b$^{\bullet-}$	C_{2h}	^{2}B$_g$	trans	11.0	0	0.776/0.751	7.4	4.7
8$^{\bullet-}$	C_2	^{2}A	cis	8.3	0	0.775/0.751	2.5	0.0

[a] All calculations performed on UB3LYP/6-31+G* geometries. "state" = electronic state symmetry. NI = number of imaginary vibrational frequencies. $<S^2>$ = spin expectation values before and after annihilation of the first spin contaminant. $<S^2>$ = 0.750 for a pure doublet. [b] For monocyclic isomers, "config" denotes the order of cis and trans C=C bonds. For bicyclic isomers, it refers to the stereochemistry at the ring juncture.

TABLE 4. Comparison of BLYP/EPR-III//B3LYP/6-31+G* a_H Values (Gauss) and Predicted Spectral Widths for Species 1$^{\bullet-}$ and 3$^{\bullet-}$−6$^{\bullet-}$ with Experimental Values Reported for 1,7-Di-*trans*-[12]annulene$^{\bullet-}$[a]

1$^{\bullet-}$ (C_1)	**3**$^{\bullet-}$ (D_2)	**4a**$^{\bullet-}$ (C_{2h})	**5**$^{\bullet-}$ (C_2)	**6a**$^{\bullet-}$ (C_1)	**6b**$^{\bullet-}$ (C_1)	expt[b]
−0.234	−0.477	0.706	0.056	0.099	−0.036	0.240
(3)	(1,2,7,8)	(1,7)	(8,11)	(10)	(8)	
−0.661	1.024	4.078	−0.671	−0.221	−0.351	0.275
(2)	(3,6,9,12)	(3,5,9,11)	(3,4)	(1)	(9)	
−1.058	3.248	−5.131	−1.218	−0.492	0.385	0.639
(8)	(4,5,10,11)	(2,6,8,12)	(7,12)	(11)	(3)	
−1.196		5.377	−1.518	−2.186	−0.696	0.884
(11)		(4,10)	(1,6)	(12)	(11)	
−1.547			−1.828	−2.293	−0.729	1.229
(12)			(9,10)	(4)	(10)	
1.681			−1.841	2.488	−1.233	1.854
(6)			(2,5)	(6)	(12)	
−1.813				−2.775	1.863	2.578
(1)				(9)	(6)	
1.959				2.947	−2.328	2.716
(7)				(3)	(5)	
−2.343				−4.311	−3.091	3.105
(10)				(5)	(4)	
3.821				−5.954	−4.981	
(5)				(2)	(2)	
4.346				−6.732	−5.202	
(4)				(7)	(7)	
4.452				20.541	22.714	
(9)				(8)	(1)	
Sum[c] = 25.11 G	Sum[c] = 19.00 G	Sum[c] = 49.00 G	Sum[c] = 14.26 G	Sum[c] = 51.04 G	Sum[c] = 43.61 G	Sum[c] = 13.52 G

[a] Numbers in parentheses denote the position(s) of the hydrogen(s) giving rise to the coupling constant. See Figure 2 for atom numbering. [b] Values obtained by simulation of the experimental ESR spectrum attributed to 1,7-di-*trans*-[12]annulene. Symmetry was unspecified, but presumably there are three other coupling constants that were too small to be observed; see ref 8a. [c] Total width of ESR spectrum (in Gauss), obtained by taking the sum of the absolute values of all a_H.

a relatively small spectral width (19.0 G), although again, coupling constants are not in agreement. (The simulated spectra for **3**$^{\bullet-}$ and **5**$^{\bullet-}$ can be found in Supporting Information.) Tri-*trans* **2**$^{\bullet-}$can be ruled out, as it has been previously characterized.[7]

Bicyclic **6a**$^{\bullet-}$ and **6b**$^{\bullet-}$ have C_1 symmetry and thus make attractive candidates, especially **6b**$^{\bullet-}$, which is the more stable conformation. However, the prediction of very large a_H values for one of the bridgehead hydrogens in each case contributes to very large total spectral widths for these two species (51.0 and 43.6 G).

With **1**$^{\bullet-}$ through **6**$^{\bullet-}$ excluded, we focused our attention on locating other possible $C_{12}H_{12}^{\bullet-}$ minima, with a goal of then determining how some of these might be connected on the $C_{12}H_{12}^{\bullet-}$ hypersurface. Figure 3 shows six other $C_{12}H_{12}^{\bullet-}$ isomers (conformational and configurational) located on the PES, along with their computed hyperfine coupling constants and total spectral widths. Their energies are in Table 3. The monocyclic entries in Figure 3 are simply different conformations of the 1,7-di-*trans*-[12]annulene radical anion. Of these, only **4b**$^{\bullet-}$ has a narrow spectral width (11.2 G) and relatively low energy (3−5 kcal/mol relative to **4a**$^{\bullet-}$). Its high symmetry (D_2) would yield a very simple spectrum (see Supporting Information), which is not observed. Thus, none of these monocyclic isomers are consistent with experiment.

Analysis of $C_{12}H_{12}^{\bullet-}$ Structure Previously Assigned to Observed ESR Spectrum. The bicyclic species in Figure 3 are heptalene-like (**7a**$^{\bullet-}$, **7b**$^{\bullet-}$, **8**$^{\bullet-}$). Loss of H_2 from any of these species would provide heptalene$^{\bullet-}$. Anion **7a**$^{\bullet-}$ is the structure for the 1,7-di-*trans*-[12]annulene radical anion previously suggested,[8a] although the bridging bond (1.588 Å long) was not depicted.[39] The computed a_H values for hydrogens at positions 1 and 7 in **7a**$^{\bullet-}$ are very large (30.3 G), consistent with sp^3 hybridized carbons at those positions.[39] The computed total spectral width for **7a**$^{\bullet-}$ is 90.2 G (BLYP/EPR-III//B3LYP/6-31+G*), much larger than the observed 13.5 G,[40] indicating that **7a**$^{\bullet-}$ was incorrectly assigned to the observed ESR spectrum.[41]

Despite the mismatch between the observed ESR parameters and those computed for **7a**$^{\bullet-}$, this structure might seem reasonable if one compared computed spin densities with empirical values (i.e., those using the McConnell relationship

(37) For **4a**$^{\bullet-}$, a state of A_g symmetry is also possible. On the basis of CASPT2(13,12)/6-31G*//CASSCF(13,12)/6-31G* results (using a full-π active space), the ^2A_g state of **4a**$^{\bullet-}$ is 7.9 kcal/mol higher in energy than the ^2B_g state. Castro, C.; Karney, W. L. unpublished results.

(38) Hammons, J. H.; Hrovat, D. A.; Borden, W. T. *J. Am. Chem. Soc.* **1991**, *113*, 4500.

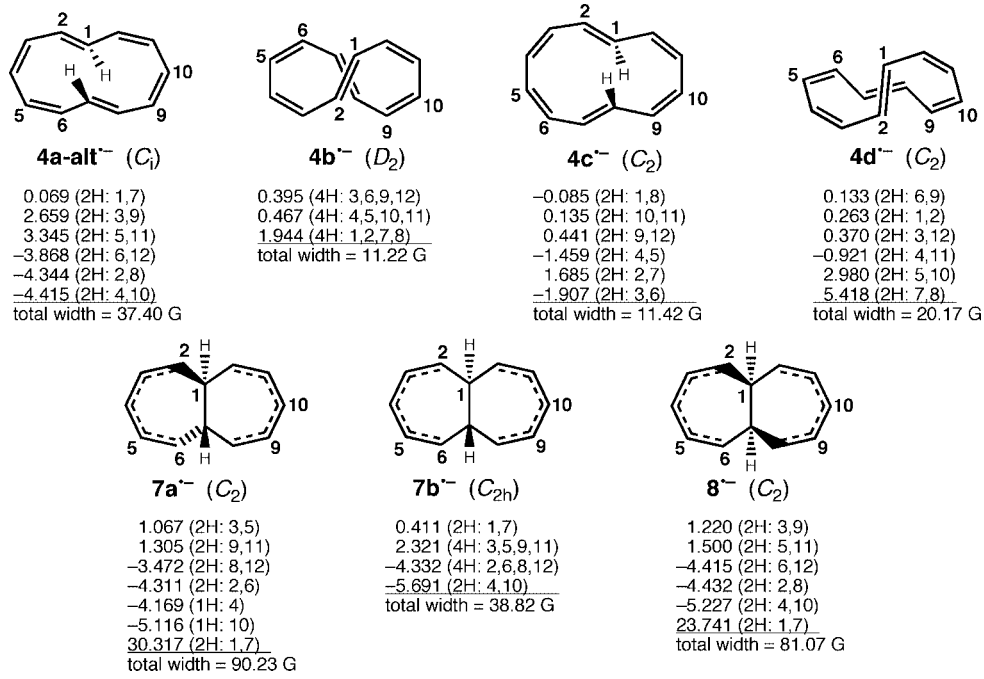

FIGURE 3. Computed a_H values (Gauss, BLYP/EPR-III//B3LYP/6-31+G*) for other conformations of **4**$^{\bullet-}$ and bicyclic isomers related to **4**$^{\bullet-}$. Also shown are computed total spectral widths. See Supporting Information for geometries and simulated spectra.

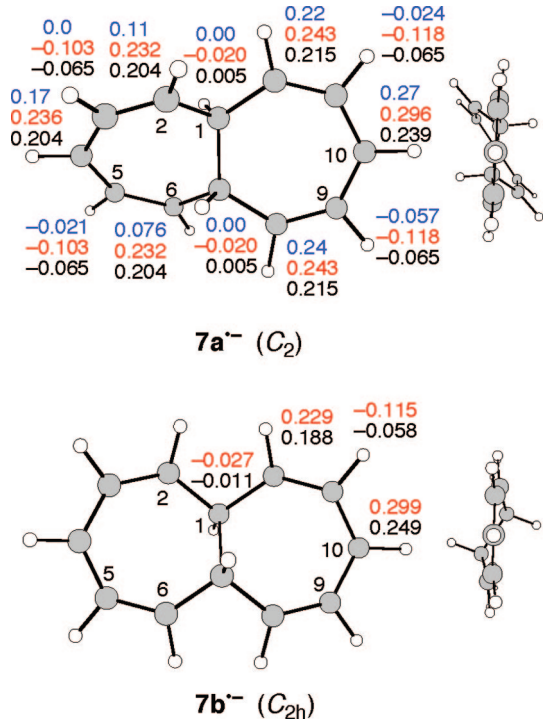

FIGURE 4. Carbon spin densities for **7a**$^{\bullet-}$ (upper) and **7b**$^{\bullet-}$ (lower). Blue, experimental values from ref 8a; red, B3LYP/6-31G*//B3LYP/6-31G*; black, BLYP/EPR-III//B3LYP/6-31+G*.

and the experimentally determined a_H values).[8a] Figure 4 shows computed carbon spin densities at both B3LYP/6-31G*//B3LYP/6-31G*[42] and BLYP/EPR-III//B3LYP/6−31+G*. The experimental spin densities are also presented.[8a] Both computed sets of data can be interpreted as agreeing reasonably well with some of the experimental values, with BLYP/EPR-III//B3LYP/6-31+G* giving closer agreement.

Compound **7a**$^{\bullet-}$ highlights a pitfall associated with using the McConnell relationship for systems with pyramidalized carbons adjacent to the π system. Despite the very small spin densities (<0.05) on the bridgehead carbons in **7a**$^{\bullet-}$, the computed coupling constants for the bridgehead hydrogens are over 30 G. We believe the origin of this large a_H value arises due to strong mixing of the bridgehead C−H σ bonding MOs with the high-lying π MOs. Figure 5 shows that the singly occupied MO (SOMO) in **7a**$^{\bullet-}$ has indeed a substantial component on the bridgehead hydrogens. The same type of interaction leads to unusually large coupling constants for the bridgehead hydrogens in most of the other bicyclic species studied here, **6a**$^{\bullet-}$, **6b**$^{\bullet-}$, and **8**$^{\bullet-}$.

Precedents for such large coupling constants in carbon-based radicals are shown in Figure 6. Hyperfine coupling constants of 35−45 G were computed (B3LYP/EPR-II) for the isomeric radicals (**9a**, **9b**, **9c**) arising from addition of the hydroxyl radical to toluene (specifically for the hydrogen at the addition site).[43] Experimental hyperfine constants for the β-hydrogens in 5,6-dihydrocytosyl radicals **10a** and **10b** range from 37 to 55 G.[44] The experimentally determined a_H for the axial β-hydrogen in the 5,6-dihydro-6-thymyl radical (**11**) is 44.0 G,[45] and this has

(39) Whether or not one chooses to draw the bridging bond, the fact remains that the two central carbons in **7a**$^{\bullet-}$ are highly pyramidalized. The sum of the bond angles (not counting the bridging bond) around these carbons is 320.4°, typical of an sp^3 carbon.

(40) At the B3LYP/6-31G*//B3LYP/6-31G* level (the method used in ref 8a), the computed spectral width for **7a**$^{\bullet-}$ is 109.6 G.

(41) If one assumes that **7a**$^{\bullet-}$ is undergoing rapid conformational automerization (in which the planar ring becomes the twisted one, and vice versa), the computed time-averaged a_H values are 1.186 G (H3, H5, H9, H11),−3.892 G (H2, H6, H8, H12),−4.643 G (H4, H10), and 30.317 G (H1, H7). These values yield a total spectral width of 90.20 G, which is still much too large relative to experiment.

(42) The spin densities in Figure 4 are significantly different from those in ref 8a. The reasons for the discrepancy are unclear.

(43) Uc, V. H.; García-Cruz, I.; Grand, A.; Vivier-Bunge, A. *J. Phys. Chem. A* **2001**, *105*, 6226.

(44) (a) Westhof, E. *Int. J. Radiat. Biol.* **1973**, *23*, 389. (b) Westhof, E.; Lion, Y.; van de Vorst, A. *Int. J. Radiat. Biol.* **1977**, *32*, 499. For calculation of hyperfine coupling constants in these systems, see: (c) Adamo, C.; Heitzmann, M.; Meilleur, F.; Rega, N.; Scalmani, G.; Grand, A.; Cadet, J.; Barone, V. *J. Am. Chem. Soc.* **2001**, *123*, 7113.

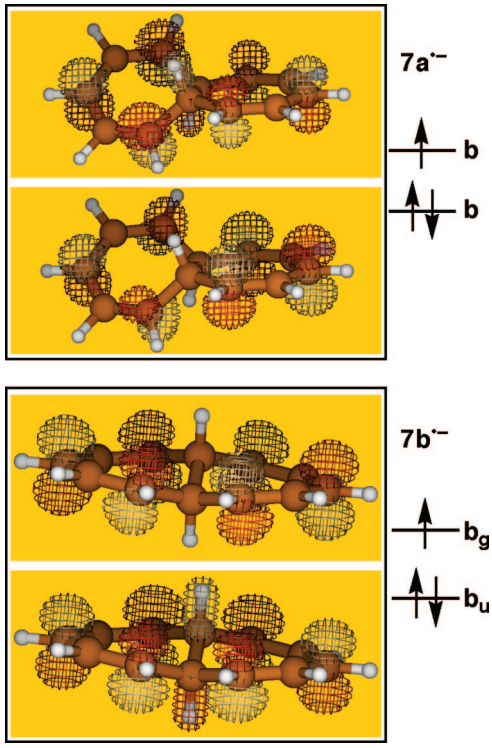

FIGURE 5. Highest occupied MOs for **7a**•− and **7b**•−, obtained from UB3LYP/6-31+G* calculations. Alpha spin MOs are depicted.

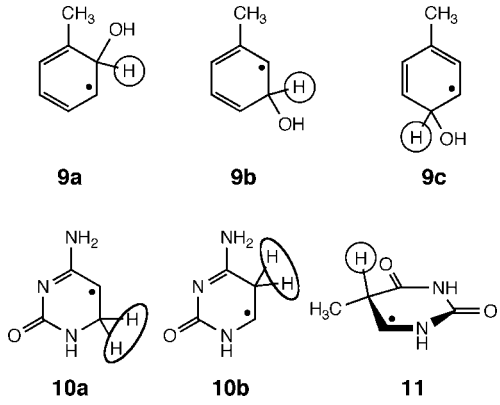

FIGURE 6. π-Radicals having β-hydrogens with large hyperfine coupling constants. The relevant hydrogens are indicated.

been reproduced computationally by Barone et al.[46] Our method affords $a_H = 45.9$ G for this system, in reasonable agreement with earlier work. Even though these precedents are not strictly hydrocarbons, they share the key structural feature of an sp^3 C−H bond adjacent to a conjugated π radical and roughly parallel to the p orbitals of the π system. Most importantly, the SOMO in all of these systems has a substantial component on the β C−H bond.

A higher-symmetry, lower-energy conformation of **7a**•−, with a longer bridging bond (1.646 Å) was located (**7b**•−, Figure 3, Table 3), suggesting that this might be the species responsible for the observed ESR spectrum. Notably, **7b**•− is the only bicyclic system we studied that has small coupling constants ($a_H = 0.41$ G) for the bridgehead hydrogens. In contrast to the other bicyclic species, in **7b**•− the MO containing the unpaired electron does *not* involve the bridgehead C−H bonds (Figure 5, lower).[47] Unfortunately, the computed a_H values indicate **7b**•− cannot account for the experimental ESR results: the computed spectral width is again too large (39 G). The computed spin densities for **7b**•− are shown in Figure 4 (bottom).

The discussion above assumes that only one $C_{12}H_{12}^{\bullet -}$ isomer contributed to the observed ESR spectrum. The discrepancy between the computed and experimental results could be due to several reasons: (1) another species not studied here is responsible for the spectrum; (2) a rapid dynamic process occurs; (3) a mixture of species contributes to the spectrum; or (4) some combination of the above. Regarding the first possibility, a likely candidate might be one with Möbius topology. This could account for the observation of more than six coupling constants, and its twisted topology should translate into a narrow spectral width. Unfortunately, all our attempts to locate such a species have not yet been successful.

Evaluation of the second and third possibilities requires some understanding of how species are connected to each other on the hypersurface. Scheme 2 depicts likely interconversions on the $C_{12}H_{12}^{\bullet -}$ PES, including plausible paths to heptalene•−. While it is tempting to try to explain the ESR spectrum by invoking a mixture of two or more species in equilibrium, the species involved must be close in energy. Not counting **2**•−, the four lowest-energy isomers (**3**•−, **4a**•−, **6b**•−, **8**•−) lie within 4.0 kcal/mol of each other (Table 3); these are shown in the box in Scheme 2. If two species are present and interconverting slowly on the ESR time scale, the observed spectral width will be that of the isomer with the larger spectral width. This rules out any species with a predicted spectral width significantly larger than 13.5 G, such as **4a**•− and **8**•−. On the other hand, if two species are rapidly interconverting, then the number of observed a_H will be equal to that predicted for the higher-

SCHEME 2

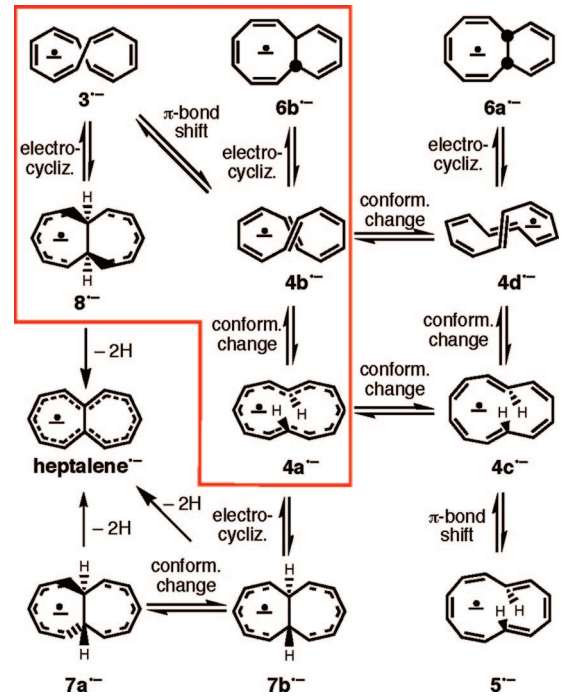

(45) Henriksen, T.; Snipes, W. *J. Chem. Phys.* **1970**, *52*, 1997.
(46) Jolibois, F.; Cadet, J.; Grand, A.; Subra, R.; Rega, N.; Barone, V. *J. Am. Chem. Soc.* **1998**, *120*, 1864.
(47) Although the highest *doubly* occupied MO does have such a component, this should not affect the a_H value.

symmetry species. None of the combinations of species would provide nine (or 12) a_H values and a total spectral width of 13.5 G. In sum, the identity of the species responsible for the experimental spectrum remains a mystery.

Analysis of ESR Spectrum Assigned to 6b$^{\bullet-}$. Interestingly, in a later paper, Stevenson et al. assigned **6b**$^{\bullet-}$ to a different ESR spectrum, observed after modifying the synthetic procedure shown in Scheme 1.[8b] It was suggested that this species arose from cyclization of neutral 1,5-di-*trans*-[12]annulene (**5**), followed by electron capture. In addition, oxidation of the observed radical anion afforded the known neutral **6b** based on NMR analysis. Our results are inconsistent with this assignment.

While the computed spectral width for **6b**$^{\bullet-}$ (43.6 G, Table 4) agrees reasonably well with the observed spectral width of 39.1 G, the computed coupling constants do not agree well with those used to simulate the experimental spectrum. In particular, the largest experimental a_H is 5.8 G, whereas the largest computed a_H is 22.7 G (Table 4). The large computed a_H arises for the same reason as discussed above for **7a**$^{\bullet-}$. The proposed C_2-symmetric structure[8b] is not a minimum but can achieve effective C_2 symmetry if there is rapid automerization. In fact, we find a very low (0.1 kcal/mol) barrier for degenerate conformational change in **6b**$^{\bullet-}$. Averaging the computed a_H gives the values −0.713, −0.795, 1.124, −2.710, −5.092, and 11.339 G, compared with the experimental values of 0.415, 0.640, 3.345, 4.277, 5.103, and 5.795 G. The computed spectral width remains essentially the same.

Although neutral **6b** was isolated and characterized after reoxidation of the radical anion,[8b] this does not necessarily mean that **6b**$^{\bullet-}$ was the species that was oxidized. It is possible that a monocyclic radical anion was oxidized to its neutral counterpart, which then rapidly cyclized to **6b**. In prior computational work, we showed that 1,7-di-*trans*-[12]annulene **4** can cyclize to **6b** with a relatively small barrier.[12] We therefore hypothesized that **4a**$^{\bullet-}$ was produced via this route and gave rise to the ESR spectrum which had been inaccurately assigned to the bicyclic radical anion **6b**$^{\bullet-}$. To assess this, we simulated the spectra for both **4a**$^{\bullet-}$ and **6b**$^{\bullet-}$ and compared them with the spectrum simulated using the published coupling constants[8b] (Figure 7). The overall appearance of the spectrum generated from **4a**$^{\bullet-}$ is clearly similar to that based on the experimental coupling constants (expt-sim). However, closer comparison reveals that the experimental spectrum has two small (<1 G) coupling constants, whereas that calculated for **4a**$^{\bullet-}$ has only one. The experimental spectrum also has significantly more lines than that of **4a**$^{\bullet-}$. Some of the deviations can be attributed to small errors in the computed coupling constants[48] or to solvent effects, and the additional lines in the experimental spectrum may be due to impurities or to a second species in equilibrium with **4a**$^{\bullet-}$. Nevertheless, of all the species we studied, **4a**$^{\bullet-}$ remains the candidate that best fits the data.

The two spectra computed for **6b**$^{\bullet-}$, one for a static structure and one assuming rapid inversion of the eight-membered ring, are very different from each other (Figure 7), highlighting the importance of accounting for dynamic processes in computing ESR spectra. Neither of these spectra matches the experimental one as well as that of **4a**$^{\bullet-}$.

Thus, the radical anion of 1,7-di-*trans*-[12]annulene (**4a**$^{\bullet-}$) may have been made, though via a synthetic sequence previously assigned to the synthesis of 1,5-di-*trans*-[12]annulene (**5**).[8b] We

(48) Small differences in coupling constants can significantly affect the overall spectral appearance, but these have little effect on total spectral width.

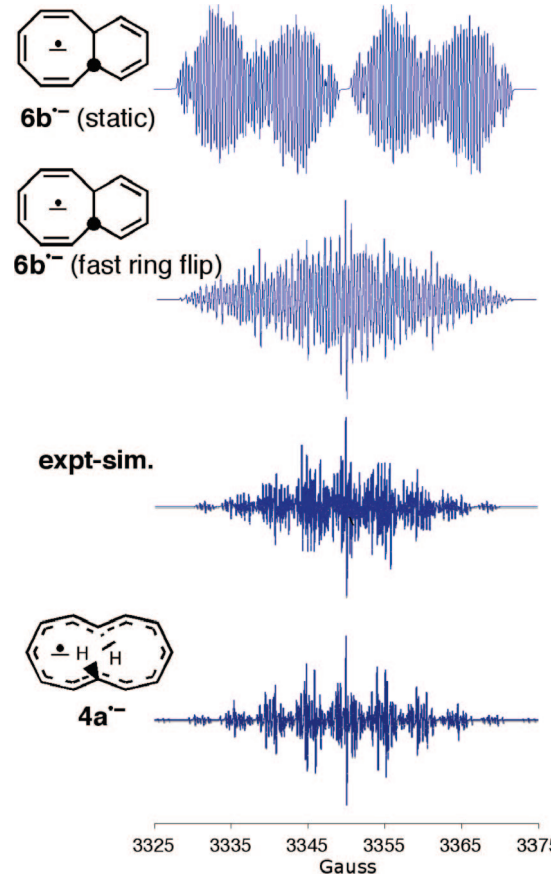

FIGURE 7. Simulated ESR spectra for $C_{12}H_{12}^{\bullet-}$ species. The spectrum labeled "expt-sim" was generated using the experimentally determined a_H values taken from ref 8b. The other three spectra were generated using hyperfine coupling constants computed in this work (BLYP/EPR-III//B3LYP/6-31+G*). See Supporting Information for enlargements of the two bottom spectra.

SCHEME 3

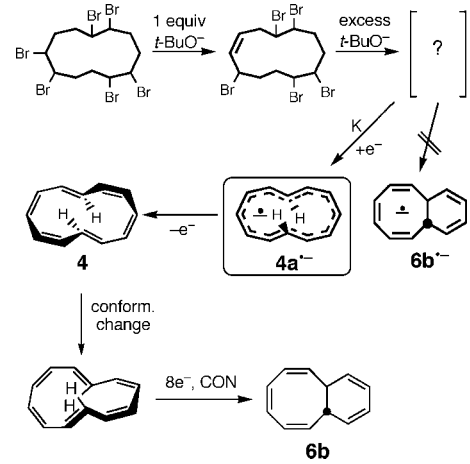

believe the ESR spectrum obtained from this synthesis was incorrectly assigned to **6b**$^{\bullet-}$. Scheme 3 summarizes this new pathway for the formation of **6b**. While the identity of the immediate precursor to **4a**$^{\bullet-}$ is unclear, we propose that neutral 1,7-di-*trans*-[12]annulene could have been formed fleetingly upon oxidation of **4a**$^{\bullet-}$, before rapidly undergoing electrocyclization.

An experimental test of the above proposal would be to reduce the observed radical anion (the carrier of the ESR spectrum

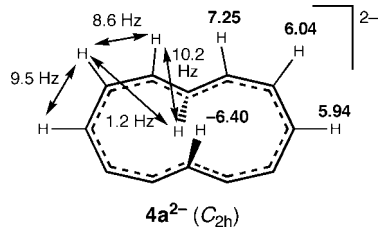

FIGURE 8. B3LYP/6-31+G*//B3LYP/6-31+G* GIAO computed proton NMR chemical shifts (bold, ppm relative to TMS) and coupling constants for the 1,7-di-*trans*-[12]annulene dianion, $\mathbf{4a}^{2-}$.

assigned to $\mathbf{6b}^{\bullet-}$) to its corresponding dianion and to obtain the NMR spectrum. The computed proton chemical shifts and NMR coupling constants of $\mathbf{4a}^{2-}$ are shown in Figure 8. Dianion $\mathbf{4a}^{2-}$ is predicted to be a minimum on the PES, with a distinct diatropic ring current (δ −6.40 ppm for the inner hydrogens). If the experimental NMR spectrum agrees with that computed for $\mathbf{4a}^{2-}$, this would support the hypothesis that $\mathbf{4a}^{\bullet-}$ was formed via the synthesis shown in Scheme 3.

Conclusion

In sum, our computational investigation of numerous $C_{12}H_{12}^{\bullet-}$ isomers leads to several key methodological and chemical findings. First, when making structural assignments for medium-sized annulene radical anions and their valence isomers, it is useful to look at computed hyperfine coupling constants in addition to computed spin densities. This ensures that very nonplanar and bridged species are adequately evaluated. Moreover, when computing a_H values, the BLYP functional is far superior to B3LYP, which performs very poorly. However, for computing this magnetic property, B3LYP geometries are adequate; the tendency of B3LYP toward "overdelocalization" is not a problem for these systems because of the stabilization gained from delocalizing the charge. UCCSD(T) results on these radical anions are prone to high-spin contamination, so restricted open-shell coupled cluster theory [RCCSD(T)] is recommended. While B3LYP and RCCSD(T) gave similar energy ordering of the monocyclic isomers, the energy differences were much larger for DFT than for RCCSD(T).

In contrast with the neutral [12]annulene PES, in which mono-*trans* **1** is the most stable [12]annulene isomer, di-*trans* isomer $\mathbf{4a}^{\bullet-}$ is predicted to be the most stable monocyclic radical anion at the RCCSD(T)/cc-pVDZ level. This unusual, completely delocalized structure appears to lack a neutral conformational counterpart. Three additional structures lie within 3 kcal/mol of $\mathbf{4a}^{\bullet-}$. On the basis of computed a_H values and simulated spectra, none of the structures considered here are consistent with the observed ESR spectrum previously assigned to the 1,7-di-*trans*-[12]annulene radical anion. However, our results suggest that an alternate synthetic route may have produced $\mathbf{4a}^{\bullet-}$ and that this species may be responsible for the ESR spectrum attributed earlier to $\mathbf{6b}^{\bullet-}$. If this hypothesis stands up, then $\mathbf{4a}^{\bullet-}$ represents the smallest bond-equalized [4*n*]annulene radical anion yet prepared. To help evaluate this hypothesis, we provide the computed ^{1}H NMR spectrum for the dianion of **4a**.

Acknowledgment. We thank Prof. Weston T. Borden for helpful discussions, and we gratefully acknowledge financial support from the Arthur Furst Scholarship Fund (M.N.B. and M.G.G.), the National Science Foundation (CHE-0553402), and the American Chemical Society Petroleum Research Fund.

Supporting Information Available: Optimized geometries for species in Figure 3, absolute energies, zero-point energies and Cartesian coordinates for all stationary points, simulated ESR spectra, and complete citation for ref 27. This material is available free of charge via the Internet at http://pubs.acs.org.

JO801249T